Short Paper

Centronuclear myopathy with abundant nemaline rods in a Japanese Black and Hereford crossbred calf

Kyohei Kamio[1)], Yoshiko Takahashi[1)], Kousuke Ishihara[1)], Akio Sekiya[1)], Satomi Kato[1)], Ikuya Shimanuki[2)], Mitugu Ide[2)], Hidefumi Furuoka[1)]

[1)]Division of Veterinary Sciences, Department of Veterinary Medicine, Obihiro University of Agriculture and Veterinary Medicine, Obihiro 080-8555, Japan; [2)]Tokachi Agricultural Mutual Aid Association, Obihiro 089-1182, Japan

Correspondence to: Hidefumi Furuoka
Division of Veterinary Sciences, Department of Veterinary Medicine, Obihiro University of Agriculture and Veterinary Medicine, Obihiro 080-8555
E-mail: furuoka@obihiro.ac.jp,
Phone: +81-155-49-5360,
Fax : +81-155-49-5359

Summary

Histopathological examination was done on skeletal and diaphragmatic muscles from 8-month-old male-crossbred beef cattle showing abnormal gait and tremor of hindlegs. The histopathology revealed extensive numbers of round fibers, and centrally placed nuclei that showed nuclear chains in the longitudinal sections, associated with interstitial fibrosis or fat tissue infiltration. In NADH-TR staining, some muscle fibers in severe lesions showed a spoke-like appearance due to the radial arrangement of sarcoplasmic strands. Also, increased NADH-TR activities in the subsarcolemmal structures, appearing as ring-like or necklace-like appearance were observed. Electron microscope revealed dilated sarcoplasmic reticulum and variably shaped electron-dense inclusions consisting of myofibrillar streaming. Another prominent feature was the existence of numerous nemaline rods within muscle fibers; nemaline rods were stained red by Gomori's trichrome. Also, immunohistochemical staining revealed that nemaline rods showed strong immunoreactivity with α-actinin and desmin antibodies. In the electron microscope, these structures were composed of dense-homogeneous material and continuous with the Z disk. Thus, the case was diagnosed as the centronuclear myopathy with increased nemaline rods.

Keywords: cattle; myopathy; centronuclear myopathy; nemaline rods

Congenital myopathies in humans are early onset neuromuscular disorders showing clinically and genetically heterogeneous characteristics. Several subtypes in the congenital myopathies have been reported based predominantly on muscle pathology (Fardeau and Tomé, 1994; North, 2008; Sewry and Wallgren-Pettersson, 2017). An inherited neuromuscular disorder, centronuclear (myotubular) myopathy, is one of the congenital myopathies showing characteristic clinical symptoms and histopathological features including significantly increased central nuclei in muscles (Jungbluth *et al.*, 2008). In humans, causative mutations in several genes have been identified that are inherited in a dominant, recessive or X-linked manner, or arise de novo (Sewry and Wallgren-Pettersson, 2017). Centronuclear myopathy has also been reported in various dog breeds: Labrador retrievers, Great Danes, and Border collie dog, including cases with known genetic mutations (Beggs et al., 2010; Böhm et al., 2013; Eminaga et al., 2012; Pelé et al., 2005). In horses, a congenital centronuclear myopathy was suspected in an Arabian-cross foal showing clinical symptoms, characteristic electromyography (EMG), and ultrastructural, histopathological changes (Polle et al., 2014).

Nemaline rods have been described as a characteristic of muscle alteration in nemaline myopathy and are considered to be derived from Z-line (Malfatti and Romero, 2016; Sewry and Wallgren-Pettersson, 2017). These structures are observed in normal myotendinous junctions, normal extraocular muscles, ageing muscle and as a minor feature in several myopathies. In animals, nemaline rods have also been reported in association with several animal myopathies including congenital myopathies in cats (Cooper et al., 1986; Kube et al., 2006), some congenital and acquired myopathies in dogs (Delauche et al., 1998; Nakamura et al., 2012), and congenital myopathy in Braunvieh and Brown Swiss crossbred calves (Hafner et al., 1996). This article describes the muscle pathology in a calf diagnosed as the centronuclear myopathy with abundant nemaline rods.

A 4-month-old male Japanese Black and Hereford crossbred calf showed with unstable gait, claudication, and sometimes tremor of the hind legs during standing. It was initially diagnosed as the disease of the limbs. No abnormalities were observed in appetite, excretion, or other general conditions including blood and serum examination; no specific treatment was done. As the disease progressed, respirations were rapid and labored. Its prognosis was diagnosed as being less favorable; thus, the animal was sedated with xylazine and euthanatized by the intravenous overdose of barbiturate at 8 months of age.

Tissue samples from visceral organs, central, and peripheral nervous system were fixed with 10 % buffered formalin and embedded in paraffin, and sections were stained with hematoxylin and eosin (HE). Skeletal muscle samples taken from whole body were frozen in liquid nitrogen, transversally or longitudinally sliced at 10 μm by cryostat and stained with HE, Periodic acid Schiff reaction (PAS), modified Gomori's trichrome, NADH-tetrazolium reductase (NADH-TR). Immunohistochemistry (IHC) was performed using anti-desmin (DAKO, Denmark; diluted 1 in 500), anti-vimentin (DAKO, Glostrup, Denmark; diluted 1 in 100), anti-α-actinin (YLEM, Roma, Italy; diluted 1 in 100), and anti-embryonic myosin (Amersham Research Products, Belmont, USA; diluted 1in 200) as the primary antibodies; horseradish conjugated peroxidase-labelled polymer (DAKO Envision Kit; DAKO) as the secondary antibody. Endogenous peroxidase activity was blocked by incubation in

H_2O_2 3% for 5 minutes at room temperature. The sections were exposed each primary antibody for 1 hour at room temperature and then incubated with the second antibody for 30 minutes at room temperature. The signals were detected using diaminobenzidine (Simple stain DAB; Nichirei, Japan) followed by counterstaining with Mayer's hematoxylin. For electron microscopy, samples from the diaphragmatic muscle and longissimus muscle (lumbar portion) were fixed with 2.5 % glutaraldehyde in 0.05 M cacodylate buffer (pH 7.4), post-fixation with osmium tetroxide, embedded in resin and processed routinely for semithin and ultrathin sectioning. Skeletal muscles obtained from clinically normal 8-month-old Holstein-Friesian cattle showing no histopathological lesions were used as control for histochemistry and IHC.

Macroscopic lesions were confined in muscles of the trunk, back, pelvic limb, and thoracic wall; and were observed symmetrically. Especially, *M. longissimus thoracis*, *M. iliopsoas*, *M. vastus medialis*, *Mm. adductores* and the diaphragmatic muscles showed severe macroscopic changes and were pale and appeared dry (Supplementary Fig. 1). No significant macroscopic lesions were observed in visceral organs, nervous system and skeleton including bone development and joint formation.

In control animal, muscles showed closely packed polygonal muscle fiber profiles and normal cytoplasmic staining in HE and modified Gomoro's trichrome staining (Supplementary Fig.2). NADH-TR and PAS staining revealed a random distribution of fibers with high and low activity depend on the presence of oxidative activity or the storage of glycogen, respectively (Supplementary Fig. 3). Immunohistochemical study using desmin and α-actinin antibodies detected no abnormal structures in muscle fibers of control animal. In affected animal, histopathological changes were observed in the skeletal muscles showing no macroscopic changes with the various degree of severity; scattering of fibers with central nuclei and scattering of small round fibers among fibers of variability in size (Supplementary Fig. 4). Histopathological features were observed in the skeletal muscles showing macroscopic lesions: the central position of nuclei in round muscle fibers associated with severe adipose tissue infiltration (Supplementary Fig. 5). In addition, marked variability in the muscle fiber size was noted with numerous hypotrophic fibers, perimysial fibrosis and increased numbers of satellite nuclei (Fig. 1). In longitudinal sections, long chains of nuclei were observed in the center of muscle fibers (Fig. 2). In NADH-TR staining, muscle fibers of affected animal revealed a spoke-like appearance because of the radial arrangement of sarcoplasmic strands (Supplementary Fig. 6). These sarcoplasmic radial strands reacted strongly with PAS and desmin immunoreactivity. Also, increased NADH-TR activities in the subsarcolemmal structures were observed as ring-like or necklace-like appearance; these ring-like structures also showed strong reactivity for PAS and desmin immunoreactivity. Diaphragmatic muscles showed the most severe histopathological lesions; almost all muscle fibers were small and round and having one or more central nuclei, indicating that those diaphragmatic muscles were immature due to a developmental problem (Supplementary Fig. 7a). In addition, increased reactivity to NADH-TR was observed in diaphragmatic muscles, especially in the central part of muscle fibers, and often surrounded by a pale halo at the periphery of the fibers (Supplementary Fig. 7b). Dark red inclusion bodies were also observed in the skeletal muscle samples stained with Gomori's trichrome method; showed the

tendency of clustering together at the center of fibers (Fig. 3). These inclusion bodies showed strong immunoreactivity to α-actinin (Supplementary Fig. 8) and desmin antibodies; however, no immunoreactivity was observed with vimentin antibody. In electron microscope, immature fibers observed in the diaphragmatic muscles showed centralized nuclei surrounded by an area devoid of myofibrils and containing glycogen granules, dilated sarcoplasmic reticulum, degenerated mitochondria, and electron-dense, variously shaped inclusions consisted of myofibrillar streaming (Supplementary Fig. 9). Ring-like or necklace-like fibers showed central area bordered by an area devoid of myofibrils and containing glycogen granules and dilated sarcoplasmic reticulum (Supplementary Fig. 10). Periphery of these fibers showed a zone with lack of myofibrils. Accumulations of numerous mitochondria localized in the center of the fibers were observed in some fibers (data not shown). The longitudinal sections having nemaline rods revealed the streaming of the electron-dense inclusions associated with myofibrillar degeneration in the center of fibers (Fig. 4). Some inclusions were regularly aligned in parallel at the corresponding position of the Z disk; the alterations were also observed at the peripheral zone of fibers, and at the disintegrated position of the Z disk. In control animal, no ultrastructural abnormalities were observed in sarcolemma, myofiber nuclei and myofibrils in the diaphragmatic muscles and longissimus muscle.

The calf investigated in this study was diagnosed as centronuclear myopathy based on the pathological characteristic observed: varying muscle fiver size, abundant centrally placed nuclei in the muscle fibers, and clinical features considering a case of suspected congenital myopathy. The macroscopic lesions in muscles could possibly be factors to cause clinical symptoms: abnormal gait, claudication and respiratory embarrassment. Both the dam and sire were clinically normal and thus it is not clear if this disorder was an inherited disease. Congenital myopathy, suspected to be inherited, has been reported in Braunvieh and Brown Swiss crossbred calves (Hafner et al., 1996). The affected calves showed rapidly progressing muscular weakness and became recumbent within 2 weeks of birth. The characteristic histological findings of skeletal muscle were intracytoplasplasmic homogeneous structures in the periphery of muscle fibers and accumulation of nemaline rods. However, the pathological features excluding nemaline rods and age of onset in these cases were clearly different from our case.

In human, in addition to the central nuclei observed by muscle biopsy, other pathological characteristics associated with gene mutations have been reported (Romero, 2010; Sewry and Wallgren-Pettersson, 2017). For example, in patients with mutations in *MTM1* gene, pale peripheral halos devoid of mitochondria, central areas devoid of organelles, central mitochondria organelles and necklace fibers were observed (Bevilacqua, et al., 2009). Radial sarcoplasmic strands surrounding the central area and necklace-like fibers are seen in patients with a *DNM2* gene mutation.

In animal cases with centronuclear myopathy, characteristic pathological features have also been reported. Subsarcolemmal ringed and central dense areas, so-called “necklace fibers”, an abnormal localization of T tubules and sarcoplasmic reticulum were observed in Labrador retriever with mutations in *MTM1* gene (Beggs et al., 2010; Cosford et al., 2008). Pathological characteristics of the inherited myopathy of Great Danes with *BIN1* gene mutation revealed dense central area in and

"spoke of wheel" appearance in the muscle fibers, ultrastructural membranous whorls, deep membrane invagination and abnormal triads in almost all muscle fibers (Böhm et al., 2013). In an Arabian-cross foal diagnosed as congenital centronuclear myopathy, necklace fibers and the dilatation of the t-tubular system, and triads filled with granular debris were observed.

Histochemical and ultrastructural characteristics observed in this study were quite similar to the specific structures reported in human and animal centronuclear myopathy. Ring like or necklace-like appearances in this case were similar to the necklace fibers or necklace-like fibers reported with the *MTM1* gene mutation in human (Bevilacqua, et al., 2009), and in Labrador retriever (Beggs et al., 2010; Cosford et al., 2008). The spoke-like appearance as the result of the radial arrangement of sarcoplasmic strands observed in NADH-TR is also similar to the radial sarcoplasmic strands surrounding the central area or "spoke of wheel" appearance reported in patients with mutations in *DNM2* and *BIN1* gene (Sewry and Wallgren-Pettersson, 2017), and great Danes with *BIN1* gene mutation (Böhm et al., 2013). Another histopathological characteristic observed here, a dark central region surrounded by a paler peripheral halo, is very similar to the reported histopathological changes in the severe neonatal *MTM1*-related centronuclear myopathy (Romero, 2010; Sewry and Wallgren-Pettersson, 2017). In addition, it is believed that this developmental arrest in myotube maturation was caused by the lack or dysfunction of the enzyme myotubularin.

In this case, gene mutations have not been investigated yet; however, protein abnormalities caused by the gene mutations could possibly contribute to the sarcoplasmic abnormalities observed here, such as myotube maturation and spoke-like and necklace-like appearance in muscle fibers. The *MTM1* gene encodes the phosphoinositide phosphatase myotubularin 1 (Laporte, et al., 1996), and the expression of *MTM1*-mutants in cultured cells was shown to result in the aggregation of cytoskeletal intermediate filaments by an unknown mechanism (Goryunov et al., 2008). It was speculated that "necklaces" was caused by the similar aggregation process of cytoskeletal components leading to alterations in the processes involved in myonuclei and organelle positioning within the fiber (Bevilacqua et al., 2019).

Nemaline rod can be distinguished from other structures that can be stained red with modified Gomori's trichrome technique, including mitochondria and cytoplasmic bodies (Nowak et al., 2013; Sewry and Wallgren-Pettersson, 2017). Ultrastrucutually, nemaline bodies are electron-dense structures, with the similar density to that of the sarcomeric Z-line, and show continuity to Z-lines. Immunohistochemically, nemaline rods reveal Z-line-related proteins including α-actinin, myotilin, desmin and actin. The acidophilic inclusions staining red with Gomori's trichrome observed in this study also expressed α-actinin and desmin immunoreactivities and ultrastructurally showed continuity to Z-line. Those morphological features observed in this case correspond closely to the morphological features of nemaline rods. Nemaline rods are the commonest pathological feature associated with nemaline myopathy; however, they occur as a nonspecific alteration in various human and animal myopathies (Banker and Engel, 1994; Delauche et al., 1996). Thus, whether the presence of nemaline rods contributes as one of the principal pathogenesis in this study is unknown. Further study to reveal gene mutations could be related to muscular disorders, and other related cases in calves are required in order to elucidate the pathogenesis of the centronuclear myopathy in cattle.

Conflict of Interest Statement

The authors declare no conflict of interest with respect to publication of this manuscript.

Supplementary data

We give the additional figures as supplementary data together with explanations.

References

Banker BQ, Engel AG (1994) Basic Reactions of Muscle, In: *Myology*, 2nd Edit., Vol. 1, AG Engel, C Franzini-Armstrong, Eds., McGraw Hill, New York, pp832-888.

Beggs AH, Böhm J, Snead E, Kozlowski M, Maurer M, et al. (2010) *MTM1* mutation associated with X-linked myotubular myopathy in Labrador Retrievers. *Proceedings of the National Academy of Sciences of the USA*, 107, 14697-14702.

Bevilacqua JA, Bitoun M, Biancalana V, Oldfors A, Stoltenburg G, et al. (2009) "Necklace" fibers, a new histological marker of late-onset *MTM1*-related centronuclear myopathy. *Acta Neuropathologica*, 117, 283-291.

Böhm J, Vasli N, Maurer M, Cowling B, Shelton GD, et al. (2013) Altered splicing of the BIN1 muscle-specific exon in humans and dogs with highly progressive centronuclear myopathy. *PLOS genetics,* 9, e1003430.

Cooper BJ, de Lahunt A, Gallagher EA, Valentine BA (1986) Nemaline myopathy of cats. *Muscle and Nerve,* 9, 618-625.

Cosford KL, Taylor SM, Thompson TL, Shelton GD (2008) A possible new inherited myopathy in a young Labrador retriever. *Canadian Veterinary Journal*, 49, 393-397.

Delauche AJ, Cuddon PA, Podell M, Devoe K, Powell HC, Shelton GD (1998) Nemaline rods in canine myopathies: 4 case reports and literature review. *Journal of Veterinary Internal Medicine*, 12, 424-430.

Eminaga S, Cherubini GB, Shelton GD (2012) Centronuclear myopathy in a Border collie dog. Journal of Small Animal Practice, 53,608-612.

Fardeau M, Tomé F (1994) Congenital myopathies. In: *Myology*, 2nd Edit., Vol. 2, AG Engel, C Franzini-Armstrong, Eds., McGraw Hill, New York, pp1487-1532.

Goryunov D, Nightingale A, Bornfleth L, Leung C, Liem RKH (2008) Multiple desease-linked myotubularian mutations cause NFL assembly defects in cultured cells and disrupt myotubularin dimerization. *Journal of Neurochemistry*, 104, 1536-1552.

Jungbluth H, Wallgren-Pettersson C, Laporte J (2008) Centronuclear (myotubular) myopathy. *Orphanet Journal of Rare Diseases*, 3, 26. doi: 10.1186/1750-1172-3-26.

Hafner A, Dahme E, Obermaier G, Schmidt P, Doll K, Schmahl W (1996) Congenital myopathy in Braunvieh × Brown Swiss calves. *Journal of Comparative Pathology*, 115, 23-34.

Kube SA, Vernau KM, LeCouteur RA, Mizisin AP, Shelton GD (2006) Congenital myopathy with abundant nemaline rods in a cat. *Neuromuscular Disorders,* 16, 188-191.

Laporte J, Hu LJ, Kretz C, Mandel JL, Kioschis P, et al. (1996) A gene mutated in X-linked myotubular myopathy defines a new putative tyrosine phosphatase family conserved in yeast. *Nature Genetics*, 13, 2, 175-182.

Malfatti E, Romero NB (2016) Nemaline myopathies: State of the art. *Revue Neurologique*, 172, 614-619.

Nakamura RK, Russell NJ, Shelton GD (2012) Adult-onset nemaline myopathy in a dog presenting with persistent atrial standstill and primary hypothyroidism. *Journal of Small Animal Practice,* 53.357-360. .

North K (2008) What's new in congenital myopathies? *Neuromuscular Disorders*, 18, 433-442.

Nowak KJ, Ravenscroft G, Laing NG (2013) Skeletal muscle α-actin diseases (actinopathies): pathology and mechanisms. *Acta Neuropathologica*, 125,19-32.

Pelé M, Tiret L, Kessler JL, Blot S, Panthier JJ (2005) SINE exonic insertion in the PTPLA gene leads to multiple splicing defects and segregates with the autosomal recessive centronuclear myopathy in dogs. *Human Molecular Genetics,* 14, 1417-1427.

Polle F, Andrews FM, Gillon T, Eades SC, McConnico RS, et al. (2014) Suspected congenital centronuclear myopathy in an Arabian-cross foal. *Journal of Internal Medicine*, 28, 1886-1891.

Romero NB (2010) Centronuclear myopathy: a widening concept. *Neuromuscular Disorders*, 20, 223-338.

Sewry CA, Wallgren-Pettersson C (2017) Myopathology in congenital myopathies. *Neuropathology and Applied Neurobiology*, 43, 5-23.

Figure legends

Fig. 1. Cryostat section of *M. vastus medialis*. The muscle fibers of the transverse section reveal varying in size and round shape with internal nuclei. Endomysial connective tissue and number of satellite nuclei are increased. HE.

Fig. 2. Cryostat section of *M. vastus medialis*. The muscle fibers of the longitudinal section show nuclear chains in the mid-portion of the fiber. Increased numbers of satellite nuclei are also visible. HE.

Fig. 3. *M. longissimus lumborum* stained with Gomori's trichrome shows variable numbers of nemaline rods. Gomori's trichrome staining.

Fig. 4. The longitudinal section of *M. longissimus lumborum* reveals the nemaline rods arise from the Z disk (arrows). Numerous nemaline rods are observed in the center of fibers, associated with or formed myofibrillar degeneration. Bar: 10μm.

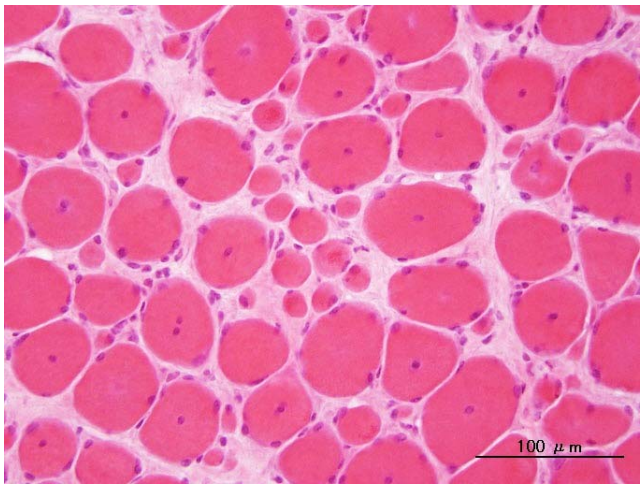

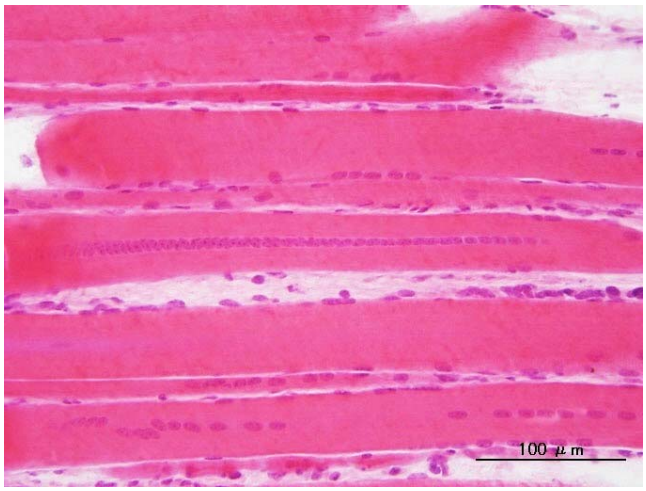

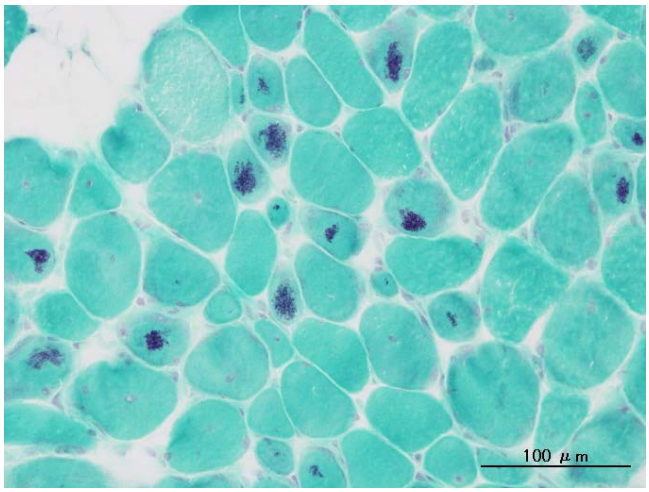

Fig. 1	Fig. 2
Fig. 3	

Fig. 4

Supplementary data-1

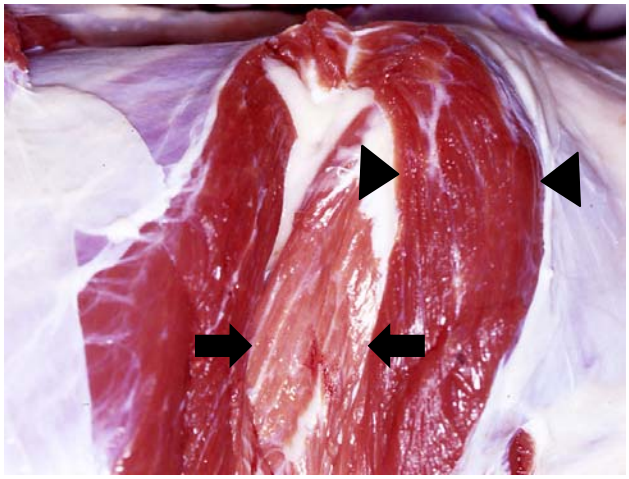

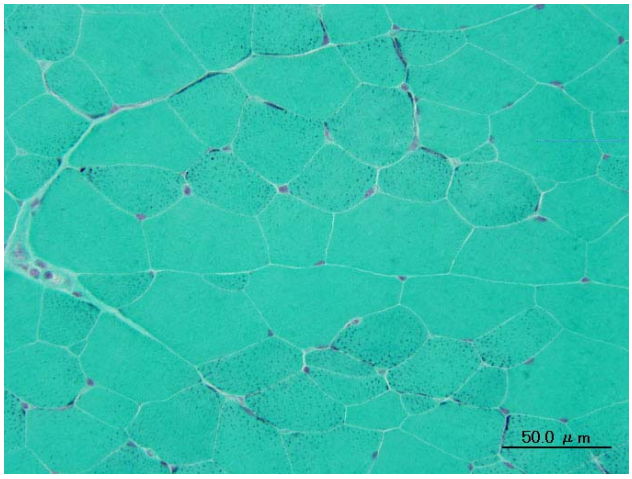

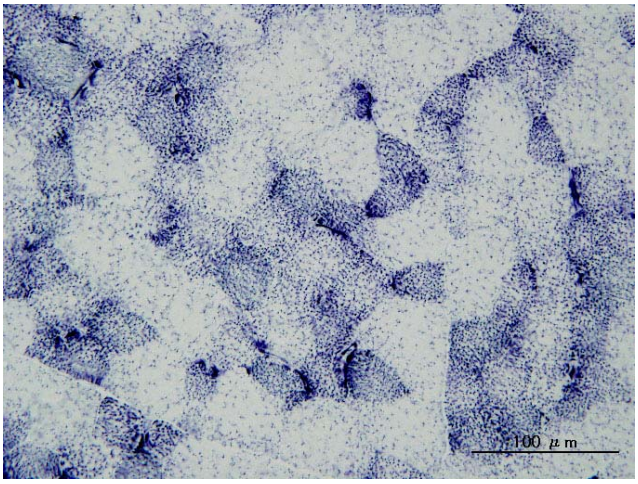

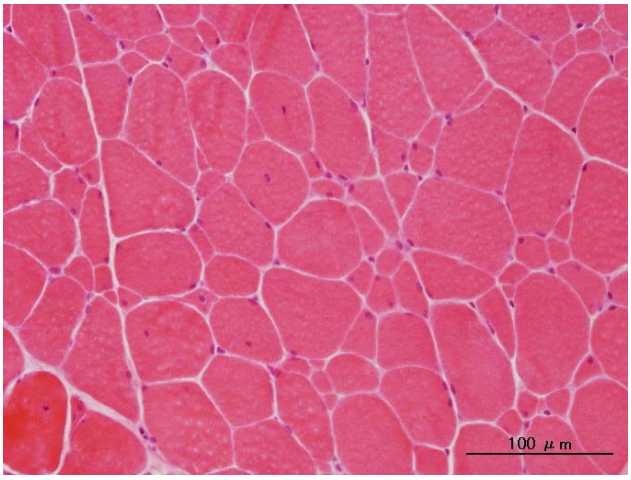

fig. 1	fig. 2
fig. 3	fig. 4

fig. 1. Gross features of the muscles of the hind legs. *M. vastus medialis* reveals pale (arrows), while the semimembranosus muscle (arrow heads) shows relatively normal color.
fig. 2. Cryostat section of *M. semimembranosus* from control animal. Normal cytoplasmic staining is pale green, and nuclei and sites of high mitochondrial density stain red. Modified Gomori's trichrome.
fig. 3. Cryostat section of *M. semimembranosus* from control animal. NADH-TR staining shows a ranom distribution of the fibers with high and low activity depend on the presence of oxidative activity.
fig. 4. Cryostat section demonstrates mild lesion and varying fiber size with internal nuclei in *M. semimembranosus*. HE.

Supplementary data-2

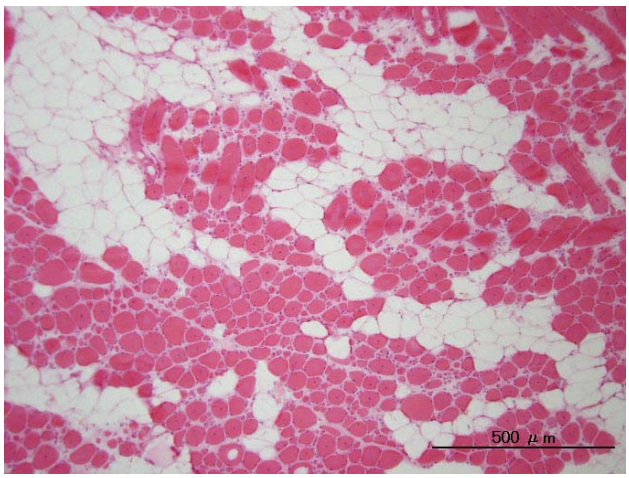

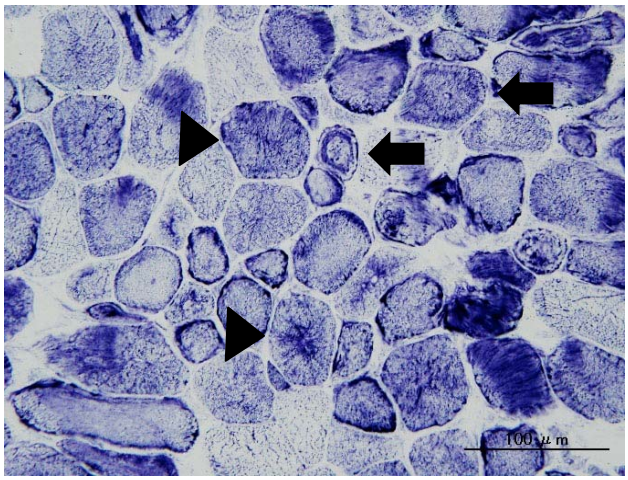

fig. 5	fig. 6

fig. 5. Cryostat section of *M. vastus medialis* shows severe lesion associated with fat tissue infiltration. HE.

fig. 6. Staining for NADH-TR reveals fibers with sarcoplasmic strands radiating from the central nucleus (arrows) and increased reactivity showing ring-like appearance (arrow heads). NADH-TR.

Supplementary data-3

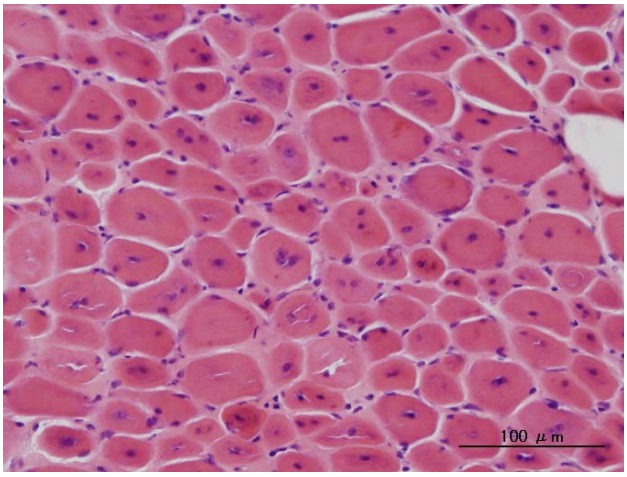

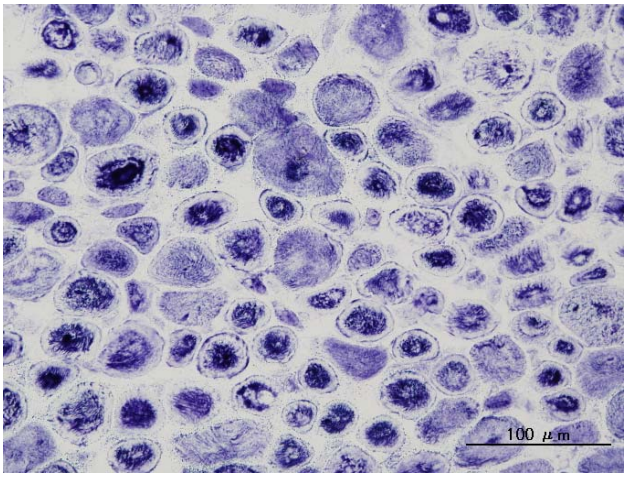

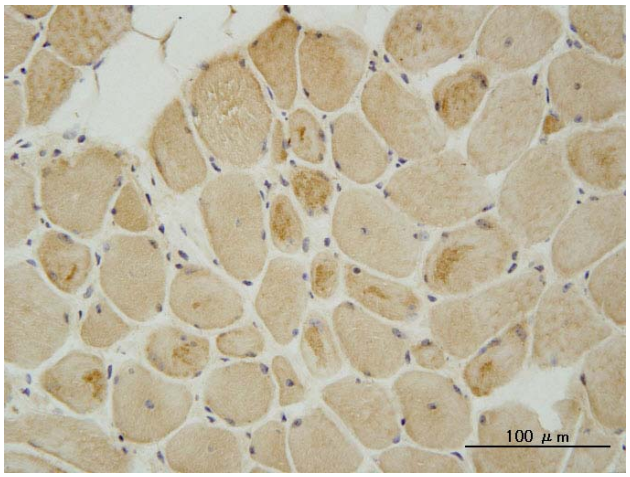

fig. 7a	fig. 7b
fig. 8	

fig. 7a, b. The diaphragmatic muscles are consisted of small rounded or polygonal fibers with several internal nuclei (a). NADH-TR staining reveals the fibers with a dark central region surrounded by pale peripheral halo (b). a: HE, b: NADH-TR.

fig. 8. *M. longissimus lumborum* shows variable numbers of nemaline rods revealed strong immunoreactivity with α–actinin antibody. IHC.

Supplementary data-4

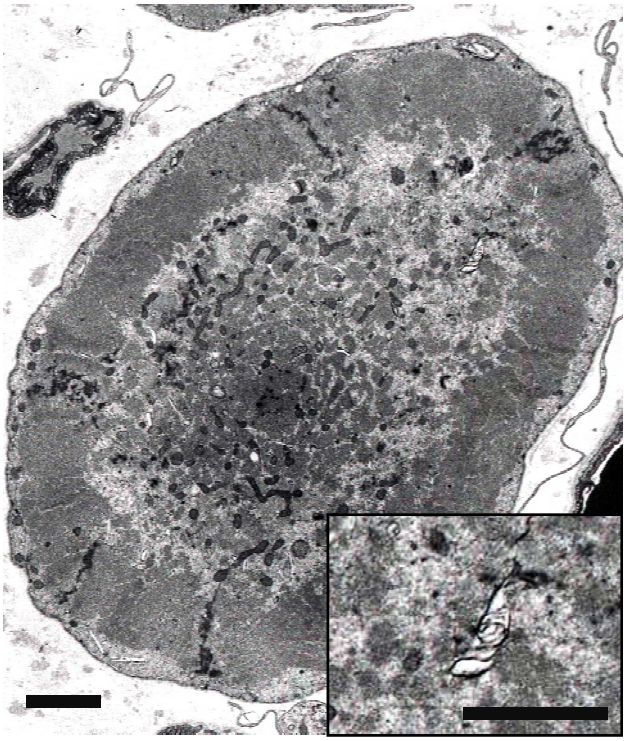

fig. 9	fig. 10

fig.9. The immature fiber of the diaphragmatic muscles shows the centrally placed nuclei surrounded by glycogen granules, and a reduction in myofibrils. Inset shows the organelles probably originating from the mitochondria. Bar: 10µm.

fig.10. Rnig-like or necklace-like fiber of *M. vastus medialis* reveals the center bordered by an area devoid of myofibrils and containing glycogen granules and dilated sarcoplasmic reticulum. Peripheral area shows a zone with lack of myofibrils. Inset shows dilated sarcoplasmic reticulum. Bar: 10µm.